NeuroImage 59 (2012) 1413–1419

Contents lists available at SciVerse ScienceDirect

NeuroImage

journal homepage: www.elsevier.com/locate/ynimg

Susceptibility induced gray–white matter MRI contrast in the human brain

Christian Langkammer [a,b,*], Nikolaus Krebs [b], Walter Goessler [c], Eva Scheurer [b], Kathrin Yen [d], Franz Fazekas [a], Stefan Ropele [a]

[a] Department of Neurology, Medical University of Graz, Austria
[b] Ludwig Boltzmann Institute for Clinical-Forensic Imaging, Graz, Austria
[c] Institute of Chemistry, Analytical Chemistry, University of Graz, Graz, Austria
[d] Institute of Forensic Medicine, University of Heidelberg, Germany

ARTICLE INFO

Article history:
Received 28 April 2011
Revised 2 August 2011
Accepted 15 August 2011
Available online 26 August 2011

Keywords:
MR phase contrast
Susceptibility contrast
Gray–white matter contrast
Brain iron
Myelin

ABSTRACT

MR phase images have shown significantly improved contrast between cortical gray and white matter regions compared to magnitude images obtained with gradient echo sequences. A variety of underlying biophysical mechanisms (including iron, blood, myelin content, macromolecular chemical exchange, and fiber orientation) have been suggested to account for this observation but assessing the individual contribution of these factors is limited in vivo.

For a closer investigation of iron and myelin induced susceptibility changes, postmortem MRI of six human corpses (age range at death: 56–80 years) was acquired in situ. Following autopsy, the iron concentrations in the frontal and occipital cortex as well as in white matter regions were chemically determined. The magnetization transfer ratio (MTR) was used as an indirect measure for myelin content. Susceptibility effects were assessed separately by determining R2* relaxation rates and quantitative phase shifts. Contributions of myelin and iron to local variations of the susceptibility were assessed by univariate and multivariate linear regression analysis.

Mean iron concentration was lower in the frontal cortex than in frontal white matter (26 ± 6 vs. 45 ± 6 mg/kg wet tissue) while an inverse relation was found in the occipital lobe (cortical gray matter: 41 ± 10 vs. white matter: 34 ± 10 mg/kg wet tissue). Multiple regression analysis revealed iron and MTR as independent predictors of the effective transverse relaxation rate R2* but solely MTR was identified as source of MR phase contrast. R2* was correlated with iron concentrations in cortical gray matter only ($r = 0.42$, $p < 0.05$).

In conclusion, MR phase contrast between cortical gray and white matter can be mainly attributed to variations in myelin content, but not to iron concentration. Both, myelin and iron impact the effective transverse relaxation rate R2* significantly. Magnitude contrast is limited because it only reflects the extent but not the direction of the susceptibility shift.

Introduction

Phase images from gradient echo sequences allow the depicting of brain structures with much more details than the corresponding conventional magnitude images (Rauscher et al., 2005). At higher field strength this phenomenon is even more pronounced and provides significantly improved contrast between gray and white matter structures (about an order of magnitude greater) (Duyn et al., 2007). These observations nourish expectations that phase imaging could serve to further improve the detection of cortical lesions in multiple sclerosis patients (Schmierer et al., 2010) and the detection of β-amyloid plaques in the cortex of transgenic mouse brains (Wengenack et al., 2011).

However, the origin of susceptibility contrast between gray and white matter is not fully understood so far. Phase and magnitude images from gradient echo sequences with longer echo times are both sensitive to the magnetic susceptibility of the underlying tissue. It has been speculated that different levels of myelin (Fukunaga et al., 2010), the relative volume and oxygenation state of blood (Lee et al., 2010a; Marques et al., 2009; Sedlacik et al., 2008), iron deposition (Fukunaga et al., 2010; Ogg et al., 1999; Yao et al., 2009), chemical exchange between water and macromolecular protons (Luo et al., 2010; Shmueli et al., 2011; Zhong et al., 2008), variations in the macromolecular mass fraction (Mitsumori et al., 2009), and the orientation of underlying white matter fibers with respect to the main magnetic field (Denk et al., 2011; He and Yablonskiy, 2009) may play a significant role for contrast mechanism. But also contributions from other trace elements such as calcium have been considered as sources of cortical susceptibility contrast (Marques et al., 2009; Yamada et al., 1996). More recent work clarified that chemical exchange between water and macromolecular protons (Shmueli et al., 2011) and also the contribution from heme-bound iron in blood (Marques et al.,

Abbreviations: MT, magnetization transfer; MTR, magnetization transfer ratio; R2, transverse relaxation rate; R2′, rf-reversible dephasing rate; R2*, effective transverse relaxation rate.

* Corresponding author at: Medical University of Graz, Department of Neurology, Auenbruggerplatz 22, 8036 Graz, Austria. Fax: +43 316 385 16808.
E-mail address: christian.langkammer@medunigraz.at (C. Langkammer).

1053-8119 © 2011 Elsevier Inc. Open access under CC BY-NC-ND license.
doi:10.1016/j.neuroimage.2011.08.045

2009; Petridou et al., 2010; Sedlacik et al., 2008) are not sufficient to explain the extent of the MR phase shifts typically observed.

Because of its well known paramagnetic effect and its abundance, iron was suggested as a major determinant of susceptibility induced contrast (Schenck and Zimmerman, 2004). However, although the effective transverse relaxation rate R2* shows a strong linear correlation with iron concentration in gray matter, this relationship is much weaker in white matter indicating that also other factors may play a dominant role (Langkammer et al., 2010; Schweser et al., 2011). In this context it was suggested that the diamagnetic effect of myelin proteins may counteract the paramagnetic effect of iron and therefore might contribute to the susceptibility induced contrast between gray and white matter (Fukunaga et al., 2010; He and Yablonskiy, 2009). Despite all these considerations, the sources of these contrasts are still a matter of debate and a validation of the underlying biophysical mechanisms is lacking.

The aim of the present study therefore was to investigate possible contributions of myelin and iron to the susceptibility induced contrast between cortical gray and white matter. As there is no in vivo method available for reliably assessing iron concentration in white matter, this study was conducted in deceased subjects shortly after death. High resolution gradient echo magnitude and phase images were acquired in the brain and then related to myelin content and chemically obtained iron concentration. The myelin content was assessed by magnetization transfer imaging (Schmierer et al., 2004). Additionally, R2 relaxation rate mapping was done to disentangle the effect of intrinsic tissue properties.

Materials and methods

Subjects

The local ethics committee approved this study and informed consent was obtained from each individual's next of kin.

Six deceased subjects (median age: 66.5 years; age range at death: 56–80 years; 2 female) with an autopsy requested by the local health authority were included in this study. Forensic pathologists examined the corpses to ensure compliance with the inclusion criteria, i.e., postmortem interval shorter than 72 h, no history of a neurological disorder or evidence of damage to the brain, and absence of ferromagnetic material.

Postmortem MRI

Corpses underwent MRI of the brain within 40 h after death at 3 T (TimTrio, Siemens Healthcare, Erlangen, Germany) using a head coil array with 12 receive channels. The subjects were kept refrigerated at 4 °C and, depending on the length of this period, the body temperature at the beginning of the acquisition varied between 11 and 24 °C.

High resolution susceptibility weighted MR images (Deistung et al., 2008) were acquired with a spoiled 3D dual echo gradient echo sequence (TR/TE1/TE2 = 39/9.2/20 ms; flip angle = 20°; FOV = 256 × 256 mm^2; in-plane resolution: 500 × 500 μm^2; 88 slices with 2 mm thickness; 2 averages; acquisition time = 17 min 27 s).

Myelin content was assessed by the magnetization transfer ratio (MTR) because it has been demonstrated that the extent of magnetization transfer between tissue water and myelin bound protons is directly coupled to the density of myelin in white matter (Schmierer et al., 2004). Magnetization transfer data was acquired with a spoiled 3D gradient-echo sequence (TR/TE = 40/7.38 ms; flip angle = 15°; FOV = 256 × 256 mm^2; in plane resolution = 1 × 1 mm^2; 44 slices with 4 mm thickness; acquisition time = 6 min 27 s) which was performed with and without a Gaussian shaped saturation pre-pulse (offset frequency = 1.2 kHz; duration = 10 ms; flip angle = 500°).

R2 relaxation data was acquired with a double-echo fast spin echo sequence (TR/TE1/TE2 = 5260/10/73 ms, FOV = 256 × 256 mm^2; in plane resolution = 1 × 1 mm^2; 30 slices with 3 mm thickness; acquisition time = 9 min 19 s).

MRI examination additionally included a standard neuroimaging protocol (FLAIR, high resolution MPRAGE sequence) to exclude subjects with acute cerebral damage. All scans were acquired in axial orientation using GRAPPA with an acceleration factor of 2 and were angulated parallel to the most inferior parts of the occipital and frontal lobes.

Autopsy and preparation of specimens

Brains were extracted at autopsy within 12 h after MRI and main supplying arteries (A. basilaris, Aa. carotides internae) were ligated using surgical fibers to prevent any formation of air bubbles and wash out of blood. Brains were examined exteriorly in detail by a forensic pathologist to exclude any findings of traumatic brain injury, cerebral bleedings, and cicatrices. Brains were fixed in a 4% phosphate buffered (pH 7.0 ± 0.5) formaldehyde solution, (Carl Roth GmbH, Karlsruhe, Germany) for 3 to 5 weeks (Yong-Hing et al., 2005). Within 4 days after extraction the formalin was exchanged to ensure sufficient fixation throughout the brains (Dawe et al., 2009). The brains were cut horizontally into 10 mm thick slices using an orientation identical to the MRI scans and to avoid contamination of the samples with iron, dissection of the tissue was done using ceramic knifes.

Tissue specimens were taken from cortical gray matter regions and from adjacent white matter regions. Fig. 1 shows a brain slice along with the positions of the dissected specimens. Given the limited number of available samples, these two regions (frontal and occipital) were selected because of their substantial variation in iron concentration

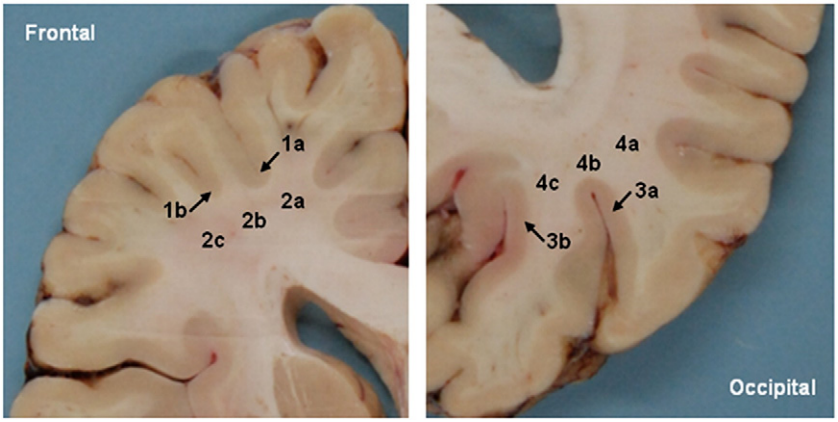

Fig. 1. Formalin fixed brain slice from a 64-years-old subject representatively showing the regions where tissue specimens were obtained for mass spectrometry. Legend: frontal cortex (1), frontal white matter (2), occipital cortex (3) and occipital white matter (4). Subunits are denoted by (a, b, c).

(Hallgren and Sourander, 1958). Gray and white matter structures were cut in two and three subunits, respectively, whereas the results of the chemical analysis were averaged for the statistical analysis. Tissue specimens were always taken from both hemispheres at identical positions.

Chemical assessment of iron concentration

Dissected tissue specimens were dried in a Gamma 1–16 LSC freeze-dryer (Martin Christ GmbH, Osterode am Harz, Germany) and aliquots of the dried tissue samples were weighed to 0.1 mg into 12 cm^3 quartz vessels. After addition of 5 cm^3 nitric acid the vessels were closed with Teflon caps and placed in the rack of a microwave-heated autoclave UltraCLAVE III (EMLS, Leutkirch, Germany). The samples were heated at 250 °C for 30 min. Iron concentrations were determined with an Agilent 7500ce inductively coupled plasma mass spectrometer (Agilent Technologies, Waldbronn, Germany) at a mass-to-charge ratio (m/z) of 56. Helium at a flow rate of 5.3 ml/min was added for reduction of the polyatomic interferences $^{40}Ar^{16}O^+$ and $^{40}Ca^{16}O^+$. The accuracy of the method was checked with the NIST RM 8414 bovine muscle (NIST, Gaithersburg, USA) and the results (69.7 ± 5.1 mg Fe/kg; n = 38) agreed well with the certified concentrations (71.2 ± 9.2 mg Fe/kg).

Image processing and analysis

Assuming monoexponential relaxation, maps of the relaxation rates R2 and R2* were calculated from the dual echo gradient echo and spin echo data, respectively. MTR maps were produced by normalizing the signal intensities obtained with MT saturation to the reference scan without MT saturation (Henkelman et al., 2001). Phase maps were obtained by unwrapping the raw phase images of the gradient echo sequence with a region growing algorithm implemented in FSL (Smith et al., 2004) followed by high pass filtering with a 8 mm Hamming kernel to remove low frequency background fields (Haacke et al., 2004). Finally, phase shift maps were calculated from the phase difference between the first and the second echoes and those maps were used in all further analyses. Exemplarily, gradient echo images (magnitude, R2* and phase shift) are shown in Fig. 2.

According to the position of the dissected tissue specimens, regions of interest (ROI) were outlined manually in a single slice of the first echo of the fast spin echo sequence, because this image series showed the best contrast between gray and white matter. Then, the outlined ROIs were transformed automatically to the registered R2*, phase shift and MTR images using an affine registration and transformation algorithm from FSL (Smith et al., 2004). Blood vessels in corpses usually contain deoxygenated blood that can lead to rapid MR signal decay in highly vascularized regions. For this reason, ROI analysis was done distantly from larger vessels. Therefore and to prevent transformation induced partial volume effects, all ROIs were manually checked after automatic affine transformation. Image analysis was performed blinded to the results of the chemical analysis.

Statistical methods

All analyses were performed using STATISTICA 7.1 (StatSoft, Tulsa, USA) and a p-value of $p<0.05$ was considered as statistically significant. Linear regression models were used to evaluate the effect of iron and myelin content on susceptibility related MRI parameters. Multivariate linear regression analysis was used to identify independent determinants of R2* and phase shifts. All statistical analyses were first carried out for all brain regions included, and then separately for gray or white matter regions only. Subjects' age was not regarded as covariates in the statistical analyses.

Results

Quantitative MRI

The results of the regional analysis of relaxation rates, MTR and phase shifts are presented in detail in Table 1. The transverse relaxation rates R2 and R2* yielded only moderate differences between cortical gray matter and white matter. In contrast, the MTR and the phase shifts were substantially different in the cortical gray compared to the adjacent white matter regions. Most remarkably, the mean phase shift in all cortical gray matter regions was positive indicating that overall paramagnetic contributions to the bulk susceptibility

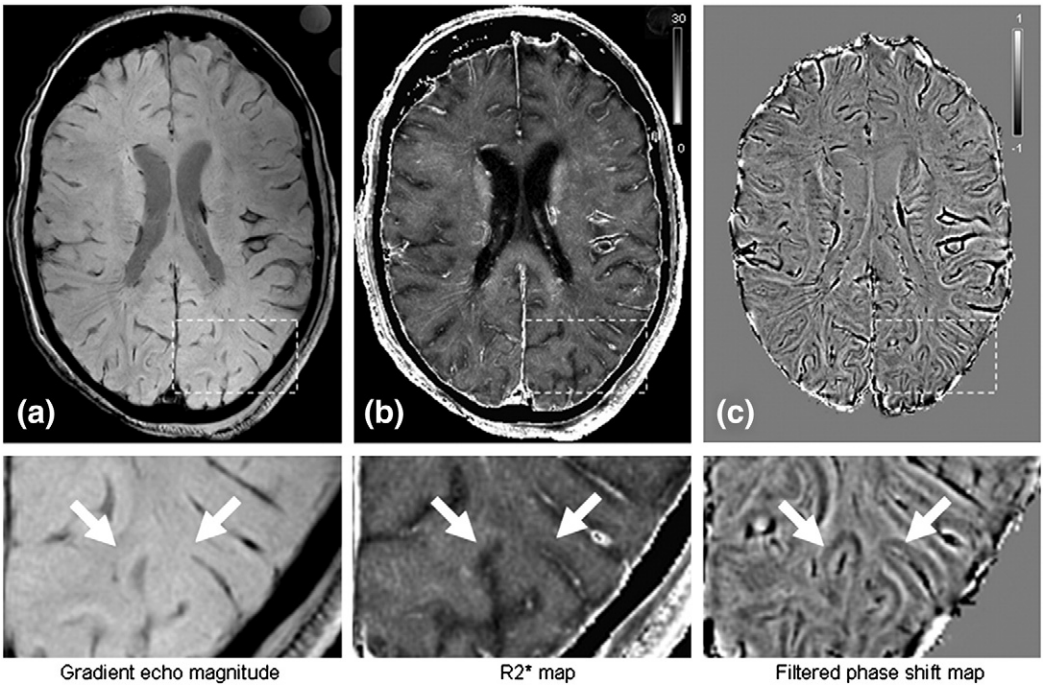

Fig. 2. MR images from an 80-years-old subject including magnified cortical region. Magnitude (a), calculated R2* (b) and filtered phase shift (c) images were acquired by a gradient echo sequence at an echo time of 20 ms. The contrast observed between cortex and white matter is substantially greater in phase (c) than in magnitude or R2* (a, b) images.

Table 1
Regional analysis of iron concentration, myelin content and corresponding measures of susceptibility.

	Iron concentration (mg/kg wet mass)		MTR (%)	R2 (s^{-1})	R2* (s^{-1})	Phase shift (Hz)
Frontal cortex	25.5 ± 6	†*29 ± 4*	27.0 ± 2.4	6.0 ± 1.1	23.9 ± 3.0	0.17 ± 0.47
Frontal white matter	44.8 ± 6	†*42 ± 8*	32.6 ± 2.4	6.8 ± 1.3	27.9 ± 2.6	−0.34 ± 0.37
Difference frontal	18.3	13	5.6	0.8	4.0	0.51
Occipital cortex	40.7 ± 10	†45 ± 7	28.1 ± 1.7	7.9 ± 0.5	26.3 ± 3.1	0.51 ± 0.34
Occipital white matter	34.3 ± 6	–	33.4 ± 2.3	7.7 ± 1.1	29.0 ± 2.2	−0.36 ± 0.35
Difference occipital	−6.4		5.3	*−0.2	2.7	0.87

Values are given in means ± 1 standard deviation unless otherwise noted.
† Iron concentrations reported by Hallgren and Sourander (1958).
* "Inverse transverse relaxation contrast".

are larger than their diamagnetic counterparts. Conversely, the mean phase shifts in white matter regions were all negative.

It should be noted that the sign of the phase is vendor specific and therefore arbitrary. Herein, positive values denote paramagnetic while negative values denote diamagnetic shifts with respect to the resonance frequency of water.

Regional variations of iron

A total of 120 specimens from six brains were analyzed with inductively coupled plasma mass spectrometry, 48 from cortical gray matter and 72 from white matter. The wet tissue weight ranged between 0.1 and 1.5 g. Mean iron concentration was lower in the frontal cortex (26 ± 6 mg/kg wet mass) than in frontal white matter (45 ± 6 mg/kg wet mass) while occipital an inverse relation was found (cortical gray matter, 41 ± 10 vs. white matter, 34 ± 6 mg/kg wet mass). For comparison, the regional iron concentrations reported by Hallgren and Sourander (1958) are also included in Table 1, where available.

Univariate regression analysis

When considering all gray and white matter samples, R2* showed a significant linear correlation with iron concentration ($r = 0.37$) and an even stronger linear correlation with the MTR ($r = 0.57$). In contrast, the MR phase shift was correlated with myelin content only ($r = -0.43$). Scatter plots of these analyses are shown in Fig. 3 and the results of all univariate regression analyses are summarized in Table 2.

When including only cortical gray matter regions, R2* showed an even stronger correlation with iron ($r = 0.42$, $p < 0.05$) which, however, was absent for the MR phase shift.

When considering only white matter regions a significant negative correlation of iron and the MTR was found ($r = -0.47$, $p = 0.02$) which is depicted in Fig. 4.

Determinants of susceptibility induced gray–white matter contrast

Multiple regression analysis revealed iron concentration and the MTR as independent predictors of the effective transverse relaxation rate R2*. In line with the univariate results, the MTR was identified as the only independent predictor of the phase shift.

Results of the multiple regression analyses as well as the regression equations are summarized in Table 3 and these results suggest that phase contrast between gray and white matter can be mainly attributed to differences in myelin content.

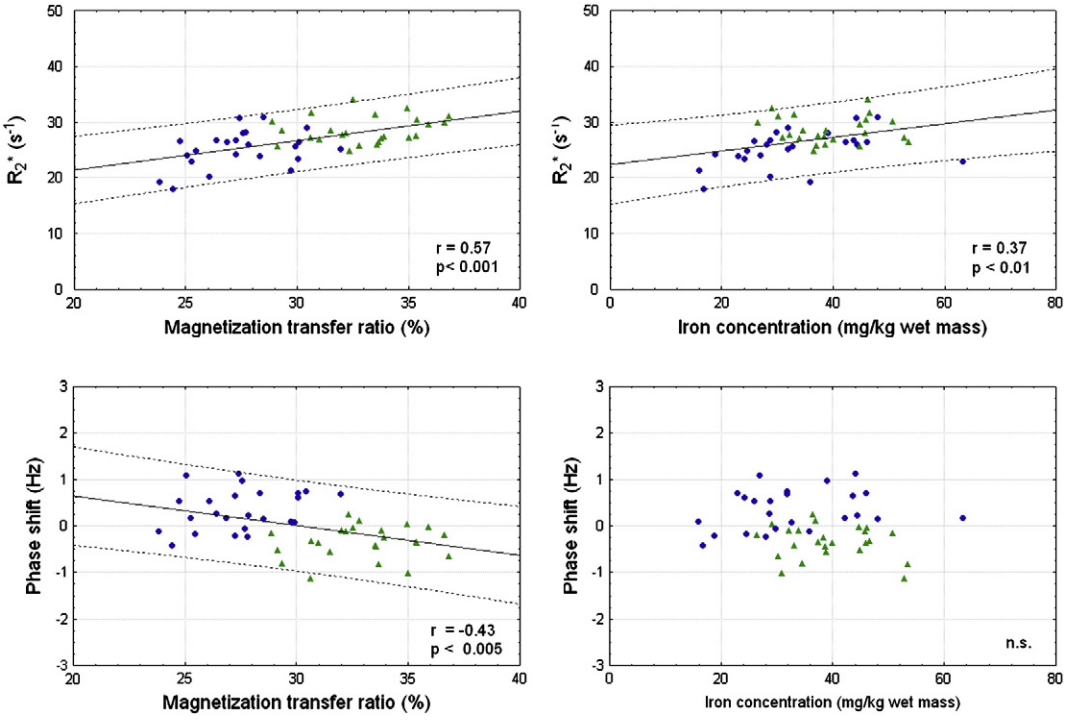

Fig. 3. Linear correlations of the MTR and iron concentration with R2* and phase shift. White matter is represented by triangles and gray matter by circles. The solid lines indicate the regression lines while the dotted lines represent the 95% confidence limits.

Table 2
Results of the univariate linear correlations (given for cortical gray and white matter combined as well as separately).

Included specimens	Dependent variable	Independent variable	r	p	Regression equation
All regions combined	R2*	Iron concentration	**0.37**	<**0.01**	y = 22.38 + 0.12x
	R2*	MTR	**0.57**	<**0.001**	y = 10.88 + 52.68x
	Phase shift	Iron concentration	−0.14	0.33	–
	Phase shift	MTR	**−0.43**	<**0.005**	y = 1.78 − 5.89x
	MTR	Iron concentration	0.13	0.35	–
Cortical gray matter	R2*	Iron concentration	**0.42**	<**0.05**	y = 21.18 + 0.12x
	R2*	MTR	0.38	0.07	–
	Phase shift	Iron concentration	0.25	0.24	–
	Phase shift	MTR	0.28	0.18	–
	MTR	Iron concentration	0.01	0.99	–
White matter	R2*	Iron concentration	−0.06	0.77	–
	R2*	MTR	0.21	0.32	–
	Phase shift	Iron concentration	−0.17	0.40	–
	Phase shift	MTR	0.12	0.59	–
	MTR	Iron concentration	**−0.47**	<**0.02**	y = 38.59 − 0.142x

p = p-value, r = Pearson regression coefficient.
Significant results are given in bold.

Discussion

In this postmortem study the susceptibility induced contributions of iron and myelin content to cortical gray and white matter MRI signal generation in unfixed brain tissue were investigated. Recent studies demonstrated that blood volume and its oxygenation state as well as chemical exchange between water and macromolecular protons are not sufficient to explain the phase contrast observed between cortical gray and white matter. However, regional iron concentrations were not included in those studies because there is no complementary in vivo technique for the assessment of iron. To overcome this limitation, in situ MRI was performed in deceased subjects shortly after death and the regional iron concentrations were determined chemically.

Determinants of susceptibility induced contrast between cortex and white matter

Linear regression analysis revealed, that the R2* relaxation rate is affected by both, significant contributions of paramagnetic iron and diamagnetic myelin where the latter was more dominant. In contrast, solely myelin content was identified as independent predictor for the phase shift. Given the fact, that both measures of susceptibility, R2* and phase shifts, are derived from the same gradient echo sequence, these observations seem unexpected at a first glance.

The phase of a gradient echo is linearly related to differences of the bulk susceptibility with respect to water and therefore can yield positive and negative values. R2* is the sum of the tissue intrinsic R2 relaxation rate and the rate R2′ which is attributed to rf-reversible field inhomogeneities as induced by iron or myelin (Yablonskiy and Haacke, 1994). As R2* reflects the net loss of spin coherence, it is not relevant whether the susceptibility difference (to water) arises from paramagnetic or diamagnetic origin. This implies that the mean bulk susceptibilities of cortical gray and white matter are of similar extent, but in opposite directions as indicated by a different sign of the acquired phase signal. An illustration of this relationship is provided in Fig. 5. The rather small differences in mean R2 and R2* rates found between cortex and adjacent white matter regions (R2 range: 6.0 to 7.7 s^{-1}, R2* range: 23.9 to 29.0 s^{-1}) are in line with these considerations as well as the large mean phase shift difference (range: −0.36 to 0.51 Hz). These observations are supported by the results of recent quantitative susceptibility mapping studies (Liu et al., 2011b; Schweser et al., 2011) and provide experimental evidence and an explanation, why the observed cortical phase contrast is superior in comparison with the magnitude contrast. Further evidence that myelin is responsible for the observed susceptibility related phase shift between gray and white matter comes from studies of the myelination process in neonates (Zhong et al., 2011) and also from transgenic shiverer mice (Liu et al., 2011a) which both offer the possibility to investigate a much broader range of myelination than in matured brains.

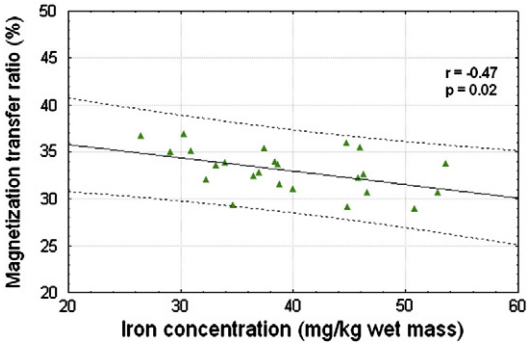

Fig. 4. The MTR showed a negative correlation with iron in white matter. The solid line indicates the regression line while the dotted lines represent the 95% confidence limits.

In this study, we used the MTR as an indirect measure for the myelin content. While this concept is commonly applied for white matter, it has not been validated for cortical gray matter so far. Basically, the two-pool model for magnetization transfer between myelin and tissue water can also be applied to cortical gray matter with the difference that myelin content is lower and T1 is higher than in white matter (Stanisz et al., 2005). The latter is responsible why the MTR in the cortex is much higher than one would expect this from the myelin content. In the context of our study this suggests that the effect of the myelin content on the susceptibility may have been underestimated in the multiple regression analysis.

R2 is correlated with iron concentration in cortical gray matter*

Given the overwhelming effects from diamagnetic myelin in comparison to paramagnetic iron in white matter, R2* and phase shift mapping cannot serve for reliably assessing iron concentrations in white matter unless the contribution of myelin is corrected for.

However, when including cortical gray matter structures only, a positive correlation between iron concentration and R2* rate was revealed. This finding is in line with other postmortem work where this relationship was found in deep gray matter structures (Langkammer et al., 2010) and is not unexpected considering the similar tissue microstructure of cortical and deep gray matter.

Relationship between myelin content and iron concentration

Another interesting finding was the significant negative correlation of iron and myelin content within white matter regions (Fig. 4). In

Table 3
Results of the multiple regression analyses for R2* and phase shift for all specimens.

Dependent variable	Independent variable	Beta	*p*	Regression equation
R2*	Iron concentration	0.30	<0.05	R2* = 0.098 * [Fe] + 48.78 * MTR + 8.46
	MTR	0.52	<0.001	
Phase shift	Iron concentration	−0.08	0.52	Phase shift = −5.73 * MTR + 1.87
	MTR	−0.42	<0.005	

p = p-value, [Fe] … iron concentration is given in mg/kg wet mass.

white matter, iron is linked with the process of myelination and was found in the proximity of myelin producing oligodendrocytes suggesting a co-localization of iron deposits with neuronal fibers (Fukunaga et al., 2010). Conversely, our results indicate an inverse relationship. However, related studies including iron chemical assessment in white matter regions (corpus callosum, frontal, temporal and occipital) also revealed that the iron concentration in the body of the corpus callosum, which is commonly considered as a region with very a high density of myelinated fibers in the human brain (Oh et al., 2006; Salat et al., 2005), is substantially smaller than in the frontal or temporal white matter (Langkammer et al., 2010). However, the cause of this inverse relationship is unclear and needs further investigations.

The role of heme-bound iron

The mass spectroscopic analysis revealed a heterogenic distribution of iron in cortical gray and white matter structures. Where available, iron concentrations were in very good agreement with values reported by Hallgren and Sourander (1958). Noteworthy, these authors excluded blood in their colorimetric measurements while in this study blood was maintained in the tissue samples during preparation. The good agreement with the values reported by of Hallgren and Sourander suggests that the total amount of heme-bound iron is marginal compared with ferritin-bound iron in the tissue specimens. To rule out that some of the heme-bound iron was washed out during fixation, we additionally performed mass spectrometric iron measurements of the formalin at the beginning and the end of the brain fixation period. However, mass spectroscopy could not proof significant iron levels in the formalin solutions.

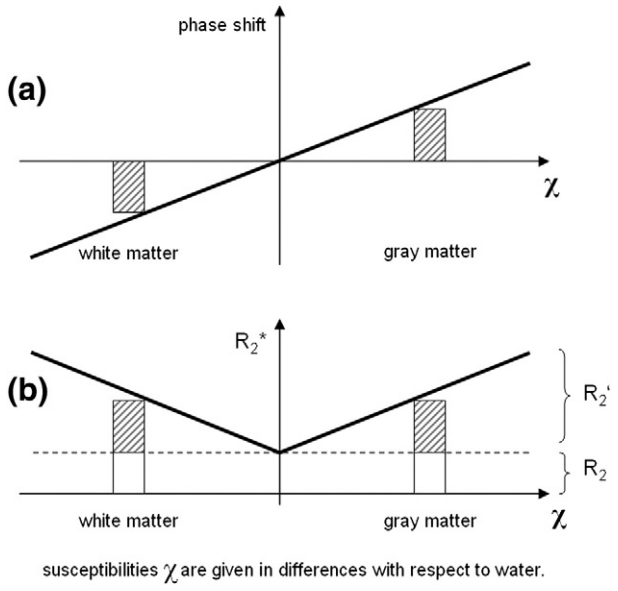

Fig. 5. MR phase shift and R2* relaxation rate as functions of the tissue susceptibility (all susceptibilities χ are given relative with respect to water). While the different susceptibilities of cortical gray and white matter cause a reversed sign of the phase shifts (a), they provide similar R2* rates (b). This may explain well the limited cortical magnitude contrast when compared to the phase contrast. (Note that the bars are not in scale with results of Table 1).

Iron is responsible for inverse transverse relaxation contrast in the cortex

Several MRI studies using T2-weighted scans have observed an unexpected behavior of contrast in the occipital lobe when compared with other cortical regions. Because it is commonly assumed that the transverse relaxation rate R2 in cortical gray matter is lower than in white matter this was entitled as "*inverse transverse relaxation contrast*" and the effect has been attributed to variations in iron (Zhou et al., 2001) and dipolar interactions (Grohn et al., 2005).

In the present study we also decided to assess R2 rates because they are intrinsically included in R2* relaxation rates (see discussion in Determinants of susceptibility induced contrast between cortex and white matter section). The R2 rates obtained were lower compared to aforementioned studies, which can be ascribed to the fact that spin diffusion occurring during the application of imaging gradients in a CPMG sequence accelerates the transverse MR signal decay. This effect is less pronounced in a dual-echo approach and in addition, intra-voxel incoherent motion is smaller in postmortem tissue.

R2 rates in frontal gray matter were lower than in white matter, while occipital R2 rates were virtually identical in cortical gray and white matter (Table 1). This can also be seen directly in the T2 weighted spin echo images, where the cortical gray–white matter contrast was less prominent in the occipital lobe (Fig. 6). Significantly lower mean iron concentrations were found in frontal cortical gray matter than in frontal white matter while this relationship was reversed occipital. When considering that R2 in white matter is not affected by iron (Langkammer et al., 2010) and changes of R2 in gray matter can be mainly assigned to variations in iron content, these results argue that iron deposition is the responsible mechanism underlying the observed loss of contrast in T2 weighted images. However, an inversion of the contrast cannot be observed in the magnitude and phase images of a gradient echo sequence (as can be seen in Fig. 2) because cortical

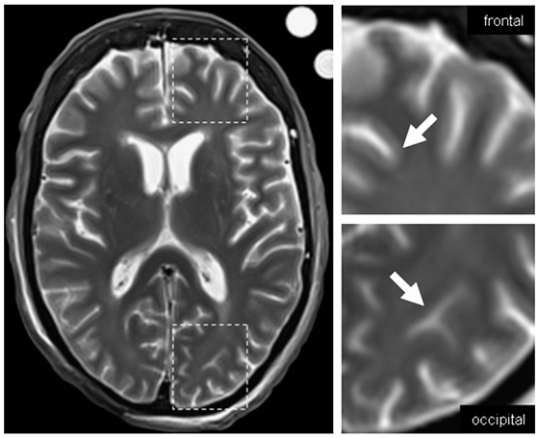

Fig. 6. The *inverse transverse relaxation contrast* can be observed in T2 weighted spin echo images. Cortical gray–white matter contrast is prominent in the frontal lobe, while it can disappear between occipital gray and white matter as a consequence of different iron levels (arrows).

susceptibility induced gray–white matter contrast is mostly driven by differences in myelin content.

Orientational dependency of myelinated fibers

In addition to theoretical considerations it was recently shown in vivo that R2* rates and phase shifts depend on the orientation of the underlying white matter fibers with respect to the main magnetic field (Denk et al., 2011; He and Yablonskiy, 2009). Also an experimental ex vivo study confirmed the dependency of gradient echo phase shift to the orientation in highly myelinated corpus callosum tissue specimens (Lee et al., 2010b). However, in our study, we did not include the orientation as a further covariate, because the selected white matter regions did not vary substantially in their fiber directions with respect to the main magnetic field. Nevertheless, the corpses included in this work were all positioned axial in the MR system – identical to clinical routine examinations – which allows a direct comparison with the transverse relaxation rates and phase shifts obtained in related in vivo studies.

Conclusion

Variations in myelin content, but not in iron concentration are responsible for the MR phase contrast observed between cortical gray and white matter. Both, myelin content and iron affect the effective transverse relaxation rate R2* independently whether the bulk susceptibility is paramagnetic or diamagnetic. Therefore, magnitude contrast is limited because it only reflects the extent but not the direction of the susceptibility shift.

Because of the lower myelin content in cortical gray matter, R2* rates can be used for the assessment of cortical iron concentrations. However, neither R2* nor phase shift mapping can serve for reliably assessing iron concentrations in the white matter unless the contribution of myelin is corrected for.

Acknowledgments

This work was supported by the Austrian Science Fund (projects P20103 and P23576). We are grateful to Michaela Soellinger (Medical University of Graz), Ferdinand Schweser (Jena University Hospital) and Daniel Kopeinigg (Stanford University) for helpful discussions and support.

References

Dawe, R.J., Bennett, D.A., Schneider, J.A., Vasireddi, S.K., Arfanakis, K., 2009. Postmortem MRI of human brain hemispheres: T2 relaxation times during formaldehyde fixation. Magn. Reson. Med. 61, 810–818.

Deistung, A., Rauscher, A., Sedlacik, J., Stadler, J., Witoszynskyj, S., Reichenbach, J.R., 2008. Susceptibility weighted imaging at ultra high magnetic field strengths: theoretical considerations and experimental results. Magn. Reson. Med. 60, 1155–1168.

Denk, C., Hernandez Torres, E., MacKay, A., Rauscher, A., 2011. The influence of white matter fibre orientation on MR signal phase and decay. NMR Biomed. 24, 246–252.

Duyn, J.H., van Gelderen, P., Li, T.Q., de Zwart, J.A., Koretsky, A.P., Fukunaga, M., 2007. High-field MRI of brain cortical substructure based on signal phase. Proc. Natl. Acad. Sci. U.S.A. 104, 11796–11801.

Fukunaga, M., Li, T.Q., van Gelderen, P., de Zwart, J.A., Shmueli, K., Yao, B., Lee, J., Maric, D., Aronova, M.A., Zhang, G., Leapman, R.D., Schenck, J.F., Merkle, H., Duyn, J.H., 2010. Layer-specific variation of iron content in cerebral cortex as a source of MRI contrast. Proc. Natl. Acad. Sci. U.S.A. 107, 3834–3839.

Grohn, H.I., Michaeli, S., Garwood, M., Kauppinen, R.A., Grohn, O.H., 2005. Quantitative T(1rho) and adiabatic Carr-Purcell T2 magnetic resonance imaging of human occipital lobe at 4 T. Magn. Reson. Med. 54, 14–19.

Haacke, E.M., Xu, Y., Cheng, Y.C., Reichenbach, J.R., 2004. Susceptibility weighted imaging (SWI). Magn. Reson. Med. 52, 612–618.

Hallgren, B., Sourander, P., 1958. The effect of age on the non-haemin iron in the human brain. J. Neurochem. 3, 41–51.

He, X., Yablonskiy, D.A., 2009. Biophysical mechanisms of phase contrast in gradient echo MRI. Proc. Natl. Acad. Sci. U.S.A. 106, 13558–13563.

Henkelman, R.M., Stanisz, G.J., Graham, S.J., 2001. Magnetization transfer in MRI: a review. NMR Biomed. 14, 57–64.

Langkammer, C., Krebs, N., Goessler, W., Scheurer, E., Ebner, F., Yen, K., Fazekas, F., Ropele, S., 2010. Quantitative MR imaging of brain iron: a postmortem validation study. Radiology 257, 455–462.

Lee, J., Hirano, Y., Fukunaga, M., Silva, A.C., Duyn, J.H., 2010a. On the contribution of deoxy-hemoglobin to MRI gray–white matter phase contrast at high field. Neuroimage 49, 193–198.

Lee, J., Shmueli, K., Fukunaga, M., van Gelderen, P., Merkle, H., Silva, A.C., Duyn, J.H., 2010b. Sensitivity of MRI resonance frequency to the orientation of brain tissue microstructure. Proc. Natl. Acad. Sci. U.S.A. 107, 5130–5135.

Liu, C., Li, W., Johnson, G.A., Wu, B., 2011a. High-field (9.4 T) MRI of brain dysmyelination by quantitative mapping of magnetic susceptibility. Neuroimage 56, 930–938.

Liu, T., Liu, J., de Rochefort, L., Spincemaille, P., Khalidov, I., Ledoux, J.R., Wang, Y., 2011b. Morphology enabled dipole inversion (MEDI) from a single-angle acquisition: Comparison with COSMOS in human brain imaging. Magn. Reson. Med. 66, 777–783.

Luo, J., He, X., d'Avignon, D.A., Ackerman, J.J., Yablonskiy, D.A., 2010. Protein-induced water 1H MR frequency shifts: contributions from magnetic susceptibility and exchange effects. J. Magn. Reson. 202, 102–108.

Marques, J.P., Maddage, R., Mlynarik, V., Gruetter, R., 2009. On the origin of the MR image phase contrast: an in vivo MR microscopy study of the rat brain at 14.1 T. Neuroimage 46, 345–352.

Mitsumori, F., Watanabe, H., Takaya, N., 2009. Estimation of brain iron concentration in vivo using a linear relationship between regional iron and apparent transverse relaxation rate of the tissue water at 4.7 T. Magn. Reson. Med. 62, 1326–1330.

Ogg, R.J., Langston, J.W., Haacke, E.M., Steen, R.G., Taylor, J.S., 1999. The correlation between phase shifts in gradient-echo MR images and regional brain iron concentration. Magn. Reson. Imaging 17, 1141–1148.

Oh, J., Han, E.T., Pelletier, D., Nelson, S.J., 2006. Measurement of in vivo multicomponent T2 relaxation times for brain tissue using multi-slice T2 prep at 1.5 and 3 T. Magn. Reson. Imaging 24, 33–43.

Petridou, N., Wharton, S.J., Lotfipour, A., Gowland, P., Bowtell, R., 2010. Investigating the effect of blood susceptibility on phase contrast in the human brain. Neuroimage 50, 491–498.

Rauscher, A., Sedlacik, J., Barth, M., Mentzel, H.J., Reichenbach, J.R., 2005. Magnetic susceptibility-weighted MR phase imaging of the human brain. AJNR Am. J. Neuroradiol. 26, 736–742.

Salat, D.H., Tuch, D.S., Greve, D.N., van der Kouwe, A.J., Hevelone, N.D., Zaleta, A.K., Rosen, B.R., Fischl, B., Corkin, S., Rosas, H.D., Dale, A.M., 2005. Age-related alterations in white matter microstructure measured by diffusion tensor imaging. Neurobiol. Aging 26, 1215–1227.

Schenck, J.F., Zimmerman, E.A., 2004. High-field magnetic resonance imaging of brain iron: birth of a biomarker? NMR Biomed. 17, 433–445.

Schmierer, K., Scaravilli, F., Altmann, D.R., Barker, G.J., Miller, D.H., 2004. Magnetization transfer ratio and myelin in postmortem multiple sclerosis brain. Ann. Neurol. 56, 407–415.

Schmierer, K., Parkes, H.G., So, P.W., An, S.F., Brandner, S., Ordidge, R.J., Yousry, T.A., Miller, D.H., 2010. High field (9.4 Tesla) magnetic resonance imaging of cortical grey matter lesions in multiple sclerosis. Brain 133, 858–867.

Schweser, F., Deistung, A., Lehr, B.W., Reichenbach, J.R., 2011. Quantitative imaging of intrinsic magnetic tissue properties using MRI signal phase: an approach to in vivo brain iron metabolism? Neuroimage 54, 2789–2807.

Sedlacik, J., Kutschbach, C., Rauscher, A., Deistung, A., Reichenbach, J.R., 2008. Investigation of the influence of carbon dioxide concentrations on cerebral physiology by susceptibility-weighted magnetic resonance imaging (SWI). Neuroimage 43, 36–43.

Shmueli, K., Dodd, S.J., Li, T.Q., Duyn, J.H., 2011. The contribution of chemical exchange to MRI frequency shifts in brain tissue. Magn. Reson. Med. 65, 35–43.

Smith, S.M., Jenkinson, M., Woolrich, M.W., Beckmann, C.F., Behrens, T.E., Johansen-Berg, H., Bannister, P.R., De Luca, M., Drobnjak, I., Flitney, D.E., Niazy, R.K., Saunders, J., Vickers, J., Zhang, Y., De Stefano, N., Brady, J.M., Matthews, P.M., 2004. Advances in functional and structural MR image analysis and implementation as FSL. Neuroimage 23 (Suppl 1), S208–S219.

Stanisz, G.J., Odrobina, E.E., Pun, J., Escaravage, M., Graham, S.J., Bronskill, M.J., Henkelman, R.M., 2005. T1, T2 relaxation and magnetization transfer in tissue at 3 T. Magn. Reson. Med. 54, 507–512.

Wengenack, T.M., Reyes, D.A., Curran, G.L., Borowski, B.J., Lin, J., Preboske, G.M., Holasek, S.S., Gilles, E.J., Chamberlain, R., Marjanska, M., Jack Jr., C.R., Garwood, M., Poduslo, J.F., 2011. Regional differences in MRI detection of amyloid plaques in AD transgenic mouse brain. Neuroimage 54, 113–122.

Yablonskiy, D.A., Haacke, E.M., 1994. Theory of NMR signal behavior in magnetically inhomogeneous tissues: the static dephasing regime. Magn. Reson. Med. 32, 749–763.

Yamada, N., Imakita, S., Sakuma, T., Takamiya, M., 1996. Intracranial calcification on gradient-echo phase image: depiction of diamagnetic susceptibility. Radiology 198, 171–178.

Yao, B., Li, T.Q., Gelderen, P., Shmueli, K., de Zwart, J.A., Duyn, J.H., 2009. Susceptibility contrast in high field MRI of human brain as a function of tissue iron content. Neuroimage 44, 1259–1266.

Yong-Hing, C.J., Obenaus, A., Stryker, R., Tong, K., Sarty, G.E., 2005. Magnetic resonance imaging and mathematical modeling of progressive formalin fixation of the human brain. Magn. Reson. Med. 54, 324–332.

Zhong, K., Ernst, T., Buchthal, S., Speck, O., Anderson, L., Chang, L., 2011. Phase contrast imaging in neonates. Neuroimage 55, 1068–1072.

Zhong, K., Leupold, J., von Elverfeldt, D., Speck, O., 2008. The molecular basis for gray and white matter contrast in phase imaging. Neuroimage 40, 1561–1566.

Zhou, J., Golay, X., van Zijl, P.C., Silvennoinen, M.J., Kauppinen, R., Pekar, J., Kraut, M., 2001. Inverse T(2) contrast at 1.5 Tesla between gray matter and white matter in the occipital lobe of normal adult human brain. Magn. Reson. Med. 46, 401–406.